The Unfolded Protein Response Regulates Multiple Aspects of Secretory and Membrane Protein Biogenesis and Endoplasmic Reticulum Quality Control

Davis T.W. Ng,* Eric D. Spear,* and Peter Walter[‡§]

*Department of Biochemistry and Molecular Biology, Pennsylvania State University, University Park, Pennsylvania 16802; and [‡]Howard Hughes Medical Institute and [§]Department of Biochemistry and Biophysics, University of California School of Medicine, San Francisco, California 94143-0448

Abstract. The unfolded protein response (UPR) is an intracellular signaling pathway that relays signals from the lumen of the ER to activate target genes in the nucleus. We devised a genetic screen in the yeast *Saccharomyces cerevisiae* to isolate mutants that are dependent on activation of the pathway for viability. Using this strategy, we isolated mutants affecting various aspects of ER function, including protein translocation, folding, glycosylation, glycosylphosphatidylinositol modification, and ER-associated protein degradation (ERAD). Extending results gleaned from the genetic studies, we demonstrate that the UPR regulates trafficking of proteins at the translocon to balance the needs of biosynthesis and ERAD. The approach also revealed connections of the UPR to other regulatory pathways. In particular, we identified *SON1/RPN4*, a recently described transcriptional regulator for genes encoding subunits of the proteasome. Our genetic strategy, therefore, offers a powerful means to provide insight into the physiology of the UPR and to identify novel genes with roles in many aspects of secretory and membrane protein biogenesis.

Key words: protein translocation • protein maturation • gene regulation • glycosylation • protein degradation

Introduction

The segregation of specific functions into discrete compartments, or organelles, is a hallmark of all eukaryotic cells. As such, maintenance of organelles and their activities are under precise regulatory control (Nunnari and Walter, 1996). Until recently, little was known regarding the mechanisms used to monitor and respond to a cell's needs for specific organelle functions. Early clues came from observations of a regulatory pathway in mammalian cells whereby two genes, *GRP78* (BiP) and *GRP94*, are induced by N-linked glycosylation inhibitors or glucose deprivation (Pouyssegur et al., 1977). Since these perturbations affect functions of the ER, it was suggested that gene activation was a consequence of ER stress. This notion was demonstrated directly through the expression of protein folding defective mutants of the influenza HA glycoprotein. In cells expressing such mutant proteins, *GRP78* (BiP) transcription is induced specifically (Kozutsumi et al., 1988). These early experiments established the existence of a signal transduction pathway between the ER and nucleus, termed the unfolded protein response (UPR)[1] (Mori et al., 1992).

The UPR is a ubiquitous mechanism observed in all eukaryotic organisms from humans to yeast (reviewed in Chapman et al., 1998; Kaufman, 1999). An important step in uncovering the mechanisms underlying the UPR came from promoter studies of the known target gene, *KAR2*. Deletion analysis revealed specific promoter elements termed UPREs (unfolded protein response elements) that are required for regulated gene activation (Mori et al., 1992; Kohno et al., 1993). The UPRE defined from yeast *KAR2* when combined with the *CYC1* TATA box is sufficient to drive the UPR-dependent expression of a heterologous reporter gene. This result was key to a genetic strategy for isolating mutants defective for signaling through the UPR (Cox et al., 1993; Mori et al., 1993). The first gene identified encodes an ER transmembrane protein with a cytosol-facing serine/threonine kinase, Ire1p (also termed

---

Address correspondence to Davis T.W. Ng, Department of Biochemistry and Molecular Biology, Pennsylvania State University, University Park, PA 16802. Tel.: (814) 863-5686. Fax: (814) 863-5876. E-mail: dtn1@psu.edu

---

[1]*Abbreviations used in this paper:* CPY, carboxypeptidase Y; ERAD, ER-associated protein degradation; GPI, glycosylphosphatidylinositol; *PER*, protein processing in the ER gene; UPR, unfolded protein response; UPRE, unfolded protein response element.

Ern1p), which acts as a sensor of the ER lumen. Through an unknown mechanism, stimuli such as accumulation of misfolded proteins cause Ire1p to oligomerize and trans-autophosphorylate as a prerequisite step for activation (Shamu and Walter, 1996). Hereafter, the mechanism of signal transduction diverges radically from paradigms derived from studies of plasma membrane receptors. Upon activation, a cytosolic nuclease domain of Ire1p excises an intron from *HAC1* mRNA (Cox and Walter, 1996; Kawahara et al., 1997), which encodes a UPRE-specific transcription activator (Cox and Walter, 1996; Mori et al., 1996). tRNA ligase then joins the two exons, thereby completing the splicing of *HAC1* mRNA by a nonconventional, nonspliceosomal mechanism (Sidrauski et al., 1996). Unspliced *HAC1* mRNA is stable in cells and initiates translation, but the presence of the intron stalls ribosomes so that no Hac1p is produced (Chapman and Walter, 1997). Removal of the intron upon UPR activation relieves the translational block to allow synthesis of Hac1p and the induction of target genes; the Ire1p-mediated splicing reaction, therefore, is a key regulatory step in the pathway.

Despite the detailed understanding of the mechanisms surrounding UPR signaling and gene regulation, the precise physiological role of the pathway has remained largely unexplored. The most extensive list of targets was assembled from yeast and includes *KAR2, LHS1, FKB2, PDI1, EUG1,* and *ERO1*. The products of these genes localize to the ER lumen and catalyze protein folding. *KAR2* and *LHS1* encode proteins with similarity to the Hsp70 class of molecular chaperones (Normington et al., 1989; Rose et al., 1989; Craven et al., 1996). *FKB2* is a prolyl isomerase homologue (Partaledis and Berlin, 1993). *PDI1, EUG1,* and *ERO1* promote disulfide bond formation (LaMantia et al., 1991; Tachibana and Stevens, 1992; Craven et al., 1996; Pollard et al., 1998). Thus, the UPR regulates the abundance of ER resident chaperones and other enzymes required for folding, assembly, and modification of secretory and membrane proteins.

The initial identification of *IRE1* as a component of UPR signaling provided additional clues. *IRE1* was first reported as a gene required for inositol prototrophy (Nikawa and Yamashita, 1992). It was later found that regulation of the inositol biosynthetic pathway requires a functional UPR (Cox et al., 1997). The observation showed that the inositol pathway interacts intimately with the UPR. Since inositol biosynthesis and other aspects of lipid biosynthesis are coregulated, these observations suggest that the UPR is involved in the regulation of membrane biosynthesis. Such a connection may serve to expand the ER, when more ER resident proteins need to be accommodated as the result of UPR induction.

Proteins that enter the ER and cannot be folded correctly, even after boosting ER folding capacity through UPR induction, are degraded. The degradation pathway, termed ER-associated protein degradation (ERAD; reviewed in Sommer and Wolf, 1997; Brodsky and Mc-Cracken, 1999), translocates misfolded proteins back into the cytosol, where they are degraded by the proteasome. Retrotranslocation (also called dislocation) is thought to utilize the same core protein complex (Sec61p and associated subunits) that forms the protein conducting channel in the translocon through which proteins are delivered to the ER lumen. Conceptually, the UPR, in its previously known scope, and ERAD provide different means of dealing with protein misfolding in the ER: the UPR by inducing enzymes thought to play a corrective role and ERAD to dispose of proteins that cannot be rescued. Here, and in a concomitant study (Travers et al., 2000), we show that the two pathways indeed are intimately linked and that the scope of the UPR encompasses many more aspects of protein maturation and ER quality control than previously appreciated.

Materials and Methods

Strains and Antibodies

Yeast strains used in this study are described in Table I. Anticarboxypeptidase Y (anti-CPY) antiserum generously provided by Dr. Reid Gilmore (University of Massachusetts, Worcester, MA). Anti-Gas1p antiserum was a kind gift of Dr. Howard Riezman (University of Basel, Switzerland). Anti-HA mAb (12CA5) was generated by Berkeley Antibody Company.

Plasmids Used in This Study

pCS15 (*SEC61, LEU2*) was provided by Dr. Randy Schekman (University of California, Berkeley, CA) and pMR713 (*KAR2, LEU2*) was provided by Dr. Mark Rose (Princeton University, Princeton, NJ).

Construction of pDN336 and pDN388. The plasmid pDN336 used as the reporter in strain DNY421 was constructed by inserting the full-length *IRE1* gene, released from pCS110 (Cox et al., 1993) as an XhoI/BamHI fragment, and the full-length *ADE3* gene, released as a BamHI/NheI fragment, into XhoI/XbaI sites of the yeast shuttle vector, pRS316 (*URA3, CEN6, ARSH4*; Sikorski and Hieter, 1989). Both the XbaI and the NheI sites were destroyed in the construction. pDN388 is similar, except that the insert is in the pRS315 vector (*LEU2, CEN6, ARSH4*; Sikorski and Hieter, 1989).

pDN390. The plasmid, pJC835, containing the *HAC1^i* gene in the shuttle vector, pRS313 (Cox and Walter, 1996), was digested with AlwNI and NgoMI to release the gene. The fragment was ligated into pRS315 digested with the same sites.

CPY*$_{HA}$ Expression Vectors. The *prc1-1* allele expresses the variant CPY* as a glycine to arginine change at position 255 (Finger et al., 1993). We constructed an HA epitope-tagged version of CPY* by site-directed mutagenesis using a PCR-based approach. The *PRC1* gene was first amplified as two fragments. The N-proximal fragment amplified with the primers 5′-CCATCGAATTCCGTATAT-3′ and the phosphorylated primer 5′-GAAATCTTGGCCCTTGTTGACG-3′ using Vent polymerase (New England Biolabs). This fragment includes the *PRC1* promoter and coding sequences to amino acid position 251. C-proximal sequences were amplified using the phosphorylated primer 5′-CACATCGCTA-GAGAATCCTACGCC-3′ incorporating a glycine to arginine change at amino acid 251 and the primer 5′-CCCTCTAGACTAACCCAAAG-AAGCGTAATCTGGAACATCATATGGGTATAAGGAGAAACC-ACCG-3′, fusing the HA epitope tag, a termination codon, and an XbaI site. The C-proximal fragment was amplified using Taq polymerase since the primer combination precluded amplification by Vent polymerase under all conditions attempted. Blunt ends were generated for this fragment using T4 DNA polymerase. The N-proximal fragment was digested with EcoRI, the C-proximal with XbaI, and both fragments ligated into the vector pDN201 (Ng et al., 1996) digested with same enzymes. The mutant gene in pDN431 was confirmed by DNA sequence analysis. A second version of the plasmid, pDN436, was constructed by releasing the CPY*$_{HA}$ gene from pDN431 as a SalI/EcoRI (blunt) fragment and ligation into the SalI/SmaI sites of pRS315 (Sikorski and Hieter, 1989).

Genetic Screen

The reporter strain for the screen was constructed by first crossing JC147 and EY0060. Diploids derived were sporulated, tetrads dissected, and haploids screened for the following genotype: *MAT**a**, ire1::TRP1, ade2, ade3, UPRE-LacZ::HIS3*. One such strain was isolated and transformed with pDN336 to create DNY421.

For mutagenesis, 50 A$_{600}$ OD units of DNY421 cells were washed once

Table I. Strains Used in This Study

Strain	Genotype	Source
W303a	*MAT***a**, *leu2-3-112, his3-11, trp1-1, ura3-1, can1-100, ade2-1*	Walter lab
EY0060	*MAT*α, *ade3*, W303 background	Erin O'Shea, UCSF
JC147	*MAT***a**, *ire1::TRP1, ura3-1, can1-100, ade2-1, leu2-3-112::LEU2-UPRE LacZ, his3-11::HIS3-UPRE LacZ*	Cox et al., 1993
JC408	*MAT***a**, *hac1::URA3, trp1-1, his3-11,-15, ade2-1, leu2-3-112::LEU2-UPRE LacZ*	Walter lab
JC409	*MAT*α, JC408 background	Walter lab
DNY70	*MAT*α, *sec62-101, ura3Δ99, leu2Δ1, trp1Δ99, ade2-101^ochre^*	Ng et al., 1996
DNY420	*MAT*α, *ire1::TRP1, ura3-1, can1-100, ade2-1, ade3, leu2-3-112::LEU2-UPRE LacZ, his3-11::HIS3-UPRE LacZ*, (pDN336)	This study
DNY421	*MAT***a**, *ire1::TRP1, ura3-1, can1-100, ade2-1, ade3, leu2-3-112, his3-11::HIS3-UPRE LacZ*, (pDN336)	This study
DNY486	*MAT***a**, *per1-1*, DNY421 background	This study
DNY499	*MAT***a**, *per1-2*, DNY421 background	This study
DNY489	*MAT***a**, *per2-1*, DNY421 background	This study
DNY491	*MAT***a**, *per3-1*, DNY421 background	This study
DNY493	*MAT***a**, *per4-1*, DNY421 background	This study
DNY478	*MAT***a**, *per4-2*, DNY421 background	This study
DNY495	*MAT***a**, *per5-1*, DNY421 background	This study
DNY497	*MAT***a**, *per6-1*, DNY421 background	This study
DNY503	*MAT***a**, *per6-2*, DNY421 background	This study
DNY501	*MAT***a**, *per7-1*, DNY421 background	This study
DNY505	*MAT***a**, *per8-1*, DNY421 background	This study
DNY507	*MAT***a**, *per9-1*, DNY421 background	This study
DNY509	*MAT***a**, *per10-1*, DNY421 background	This study
DNY484	*MAT***a**, *per10-2*, DNY421 background	This study
DNY488	*MAT***a**, *per11-1*, DNY421 background	This study
DNY470	*MAT***a**, *per12-1*, DNY421 background	This study
DNY472	*MAT***a**, *per13-1*, DNY421 background	This study
DNY475	*MAT***a**, *per14-1*, DNY421 background	This study
DNY479	*MAT***a**, *per15-1*, DNY421 background	This study
DNY481	*MAT***a**, *per16-1*, DNY421 background	This study
DNY523	*MAT*α, *per1-1*, W303 background	This study
DNY540	*MAT***a**, *per15-1*, W303 background	This study
DNY563	*MAT***a**, pDN431, W303 background	This study
DNY572	*MAT***a**, *cue1::TRP1*, pDN431, W303 background	This study
ESY157	*MAT*α, *ire1::TRP1*, pDN431, W303 background	This study
ESY158	ESY157 with pMR713 (*KAR2*)	This study
ESY159	ESY157 with pCS15 (*SEC61*)	This study

in sterile water and resuspended in 25 ml 0.9% KCl. With constant stirring, the cells were given four 30-s pulses of short wave UV light from a source mounted 15 cm above. After each pulse, an aliquot was removed, a portion serially diluted, and spread onto YPD plates to determine the kill rate. The remainder of each aliquot was pelleted and resuspended in 10 ml YPD media and allowed to recover for 18 h on a roller drum. All procedures to this point were performed in a darkroom and incubations at 30°C. Cells receiving a UV dose of 120 s resulted in a kill rate of 62% and were used for the screen. Mutagenized cells were spread onto YPD plates lacking additional adenine. Nonsectoring colonies were picked and rescreened by restreaking for single colonies (see Results for specific numbers). Isolates were backcrossed to DNY420 and recessive mutants determined by the restoration of the colony sectoring phenotype of their respective heterozygote diploids. Tetrad dissection was performed to determine the allelic complexity of the mutants. Only those exhibiting a 2:2 segregation pattern indicating a single mutant gene were continued. All strains were backcrossed at least twofold before further analysis.

Complementation tests were performed to determine the number of genes represented in the initial group of 20. Complementing strains were scored as those giving rise to colony sectoring diploids. However, before the completion of all possible crosses, many strain combinations gave rise to nonsectoring diploids indicating noncomplementation and therefore suggesting different alleles of the same gene. Upon tetrad analysis of the diploids, it was determined that, in most cases, mutant alleles were unlinked. The criterion for linkage was 4:0 segregation of mutant to wild-type spores. Tetrad analysis was performed for all possible crosses for the assignment of linkage groups.

Cloning and Identification of PER Genes

Two general approaches were employed to clone *PER* (protein processing in the ER) genes. The first takes advantage of the counterselectable

marker, *URA3*, contained in the pDN336 (Boeke et al., 1984). Since the growth of *per* mutants are dependent on the *IRE1*, cells losing pDN336 fail to grow on media containing 5-fluoroorotic acid (5-FOA). Complementation of mutant alleles alleviates the requirement for *IRE1* and thus allows for selection of complementing plasmids from genomic libraries. The *PER5* and *PER8* genes were cloned using this first approach.

Mutant cells were transformed with a yeast genomic library based on the multicopy YEp13 vector (Lagosky et al., 1987). After transformation, the cells were grown overnight in SC-Leu media allowing transformants receiving complementing plasmids to lose pDN336. Transformants were later plated and incubated on SC-Leu media containing 5-FOA (1 mg/ml) at 30°C. Plasmids were recovered from 5-FOA resistant isolates by zirconium bead disruption and purification using the Wizard Miniprep kit (Promega). Plasmid amplification was performed after transformation into bacterial DH5α cells. Retransformation of the recovered plasmids into the respective mutant strains was typically carried out to assess complementation of the sectoring phenotypes. Although this approach worked well for *PER5* and *PER8*, it was less successful for other strains attempted. The high incidence of false positives due to plasmids carrying truncated *IRE1* contained in the library added an additional layer to the procedure that was overly time consuming.

The second approach scored for complementation of the sectoring phenotype using a low copy genomic library (used for cloning of *PER2*, *PER4*, *PER13*, and *PER16*). The library, based on YCp50 (Rose et al., 1987), required that the reporter pDN336 be swapped for pDN388 to be compatible. Mutant strains transformed by the library were spread onto SC-Ura/adenine-limiting (6 μg/ml) plates at low density (400 cfu/plate) to develop the colony color phenotype. Typically, between 10,000 and 25,000 transformants were screened for restoration of sectoring. Positives were cured of the reporter and complementing plasmids were recovered as described above. Recovered plasmids were transformed back into the respective mutant strains to confirm complementation.

For all clones, DNA sequence analysis was performed to determine the identity of inserts (Nucleic Acid Facility, Pennsylvania State University, University Park, PA). The sequences of vector/insert junctions were obtained using the primers N168 (5′-CGCTACTTGGAGCCACTATC-GAC-3′) and N169 (5′-ATCGGTGATGTCGGCGATAT-3′). Junction sequences were submitted to the *Saccharomyces* Genome Database (http://genome-www.stanford.edu/Saccharomyces/) to obtain complete insert sequences and identities of open reading frames. The insert sequences were used to facilitate deletion mapping using standard recombinant DNA methods to determine specific complementing genes. Subclones of genes derived from the high copy library (YEp13) were inserted into centroplasmic plasmids to assess complementation.

Cell Labeling and Immunoprecipitation

Typically, 3 A_{600} OD units of log phase cells were pelleted and resuspended in 0.9 ml of SC media lacking methionine and cysteine. After 30 min of incubation at the appropriate temperature, 150 μCi of [^{35}S]Met/Cys (Pro-mix; Amersham Pharmacia Biotech) is added to cells for 5 or 10 min. A chase, where appropriate, was initiated by adding cold methionine/cysteine to a final concentration of 2 mM. Cell labeling/chase was terminated by the addition of trichloroacetic acid to 10%. Cells were homogenized by the addition of 0.4 ml of 0.5-mm zirconium beads, followed with agitation in a Mini-bead beater cell disrupter (Biospec Products). The homogenate was transferred to a fresh tube and pooled with a subsequent 10% TCA bead wash. After centrifugation, the TCA precipitate pellet was resuspended in 120 μl of IPS II (100 mM Tris base, 3% SDS, 1 mM PMSF) and heated to 100°C for 5 min. Insoluble debris was pelleted and 40 μl of the detergent lysate was added to 560 μl IPS II (1% Triton X-100, 50 mM Tris, pH 7.5, 1 mM PMSF, 1 μl yeast protease inhibitor cocktail; Sigma-Aldrich) and the appropriate antiserum. After a 2-h incubation at 4°C, the sample was centrifuged for 10 min at 16,000 *g* and the supernatant transferred to a fresh tube containing protein A–Sepharose beads. The tube was rotated for 30 min and washed three to five times with IPS I (0.2% SDS, 1% Triton X-100, 50 mM Tris, pH 7.5) and once with PBS. Immunoprecipitated proteins were eluted with gel sample buffer, separated by gel electrophoresis, and visualized by autoradiography.

In pulse-chase assays to determine protein stability, immunoprecipitations were normalized by measuring TCA-precipitable counts using an LS5801 scintillation counter (Beckman Coulter) and adjusting lysates for equal counts.

Northern Blot Analysis

Preparation of RNA, gel electrophoresis, blot transfer, and probing were performed as described in Cox and Walter (1996). RNA from UPR-induced cells were treated for 60 min with 2.5 μg/ml tunicamycin (Sigma-Aldrich) before RNA isolation. All templates for probes were prepared by PCR amplification of genomic DNA. Probes were prepared by random primer extension labeling using [^{32}P]α-dCTP. The *ACT1* template is a 600-bp fragment corresponding to the 3′-end of coding sequences. The *KAR2* template is a 600-bp fragment corresponding to the 5′-end of coding sequences. Two *RFT1* templates were prepared and used independently. One includes 600 bp of the 5′-coding sequences and the other includes 700 bp of the 3′-coding sequences.

Results

Genetic Screen

We devised two complementary approaches to identify in an unbiased way cell functions that are regulated by or are dependent on the UPR. First, we used whole genome microarray analysis to directly identify UPR target genes (Travers et al., 2000). This approach allowed us to define the transcriptional scope of the UPR. Second, we devised the genetic screen that is described here in which we isolated mutants that are dependent on UPR activation for viability. This second approach aims to highlight physiologically relevant functions that connect with the UPR. The feasibility of this approach was suggested by the observations that genes mediating the UPR are nonessential

(Cox et al., 1993; Mori et al., 1993), yet display synthetic lethality (that is, cell inviability caused by the combination of two nonlethal mutations) with two known target genes (*KAR2* and *LHS1*; Craven et al., 1996; Sidrauski et al., 1996). In both *kar2* and *lhs1* mutants, the UPR is constitutively activated, which must allow the cell to compensate for the loss of the function of these genes. In principle, genetic and microarray analyses should be complementary, as some functions that are dependent on or affected by UPR activation may not be transcriptional targets of the pathway.

We performed the screen using a yeast colony color sectoring assay (Koshland et al., 1985). Yeast cells harboring an *ade2* mutation give rise to red colonies when grown on media limiting for adenine. If a strain contains both mutant *ade2* and *ade3* alleles, the red pigment is not synthesized, and colonies are white. We constructed an *ade2 ade3* mutant strain that is deleted for *IRE1* (DNY421, Table I). This strain grows well on rich media. In addition, we constructed a centromeric reporter plasmid, pDN336, containing *IRE1* and *ADE3*, which was transformed into DNY421 cells. Since *ADE3* and *IRE1* are not essential, the plasmid is lost at a frequency of $\sim 10^{-2}$ per cell division (Guthrie and Fink, 1991). For this reason, DNY421 cells gives rise to red and white sectored colonies, reflecting a mixed population of cells with and without the plasmid. Because *IRE1* is required for activation of the UPR pathway, mutants that require UPR activation for growth cannot lose the *IRE1*-bearing plasmid and hence, are expected to give rise to red nonsectored colonies.

DNY421 cells were mutagenized with ultraviolet light to 62% lethality. We screened $\sim 50,000$ colonies and isolated 101 nonsectoring and normally growing colonies. Of these, 40 were backcrossed to the parental strain, yielding 32 recessive, 2 dominant, and 6 sterile isolates. The dominant and sterile mutants were discarded. Heterozygous diploids generated from recessive mutants were sporulated and subjected to tetrad analysis to determine the segregation patterns. Of the diploids, 25 were sporulation-competent. Of those, 15 segregated 2:2 with a synthetic lethal phenotype and 5 with a synthetic negative growth phenotype (spores containing both mutations were viable, but displayed severely reduced growth rates), indicative of a single gene being responsible for the mutant phenotype. Of the remaining mutants, five exhibited other patterns and were discarded.

When crossed to each other, many of the mutants exhibited partial sectoring phenotypes that precluded clear determination of complementation. This was not a general effect of ploidy since all 20 mutants, when crossed to the parental strain, formed sectored colonies unambiguously. Further analysis demonstrated that most mutant genes are unlinked. These observations suggest some combinations of mutations display the genetic interaction termed unlinked noncomplementation. Although the significance for this group remains to be determined, unlinked noncomplementation has been used to help identify genes of the same function or pathway (Stearns and Botstein, 1988). To group the 20 mutants, we crossed individual mutant strains and systematically subjected the resulting diploids to tetrad analysis. Most crosses failed to display linkage between the mutant alleles, indicating that the mutations

Table II. Summary of per Mutant Characterization

Allele	Gene	Temperature conditional phenotype	Interaction with Δire	Protein processing defect	Suppressing by Hac1[i]p
per1-1		ts	SN	Gas1p	No
per1-2			SN		Yes
per2-1	MCD4[‡]	ts	SL	Gas1p	Yes
per3-1			SL	Glycosylation	Yes
per4-1	LHS1[‡]		SL		Yes
per4-2	LHS1[‡]	cs	SL		Yes
per5-1	RFT1[‡]		SL	Glycosylation	Yes
per6-1			SL	Glycosylation	Yes
per6-2		ts	SL	Glycosylation	Yes
per7-1			SL	CPY*HA degradation	Yes
per8-1	SON1	cs	SL	CPY*HA degradation	Yes
per9-1			SL	Gas1p/CPY*HA degradation	Yes
per10-1			SL		Yes
per10-2			SL		Yes
per11-1			SN		Yes
per12-1		ts	SL	Glycosylation	Yes
per13-1	GPI10	ts	SN	Gas1p/CPY*HA degradation	Yes
per14-1			SL	Glycosylation	Yes
per15-1		ts/cs	SL	Gas1p	No
per16-1	UBC7[‡]		SN	CPY*HA degradation	Yes

per mutant allele designations listed with corresponding gene names, if known. ts, Temperature-sensitive: impaired or no growth at 37°C; cs, cold-sensitive: impaired or no growth at 16°C; SL, synthetic lethal: mutation is lethal in combination with Δire1, as determined by tetrad analysis; SN, synthetically negative: mutation causes severely impaired growth in combination with Δire1, as determined by tetrad analysis.
[‡]Denotes genes as UPR-inducible, determined by Northern analysis or genomic microarray analysis (Travers et al.,2000).

were in different genes. This analysis defined 16 linkage groups indicating at least as many genes (Table II). We refer to the genes defined by the mutants as *PER* (protein processing in the ER) because most mutant alleles can be shown to affect various aspects of ER protein biogenesis and quality control (see below). The high fraction of *per* mutants represented by a single allele indicates that the screen is far from saturated.

To establish *PER* mutants as tools to study the functional role of the UPR, we next assessed their physiological relevance. To this end, we required two criteria to be met: activation of the UPR pathway should alleviate the synthetic growth defect caused by the mutation, and the mutants should exhibit a constitutive activation of the UPR. To address the first criterion, we activated the UPR constitutively by expression of the Hac1p transcriptional activator (Cox and Walter, 1996). We constructed a plasmid, pDN390, carrying *HAC1[i]* (*HAC1* deleted of its intron) and transformed it into each *per* mutant (Δire1 cells covered by pDN336 bearing wild-type *IRE1*). Cells were then scored for improved growth after loss of pDN336, obtained by screening for white, nonsectoring colonies. Using these criteria, all but two mutants (*per1-1* and *per15-1*) could be relieved of the requirement for *IRE1* function by directly activating the pathway (Table II). After crosses of the two remaining mutants (DNY523 and DNY540) with Δ*hac1* cells were sporulated, however, tetrad analysis revealed clear synthetic negative phenotypes for both mutants (data not shown). Thus, taken together, the results indicate that the synthetic defect of all 16 *per* mutants is due to the loss of the UPR pathway, rather than to the loss of a yet uncharacterized function of *IRE1* unrelated to UPR signaling.

To address the second criterion for physiological relevance, we determined the extent of constitutive UPR activation in mutant cells. The parental strain (DNY421) used in this study contains a genomic copy of a *lacZ* reporter gene fused to a minimal UPR promoter (Cox et al., 1993). Thus, β-galactosidase activity can be used to monitor activation of the pathway. Mutant cells were grown to early log phase, and cell extracts were prepared to measure β-galactosidase activity with the substrate 2-nitrophenyl-β-D-galactopyranoside (Cox et al., 1993). As shown in Fig. 1, with the exception of *per16-1*, all *per* mutants express β-galactosidase activity above wild-type levels, indicating induction of the UPR. Interestingly, the degree of UPR induction among the mutants varies widely, indicating that the UPR can be gradually modulated depending on the physiological needs of the cell.

Functions of PER Genes

Having satisfied the criteria for a physiological relationship, we next assessed functional defects of *per* mutants. To this end, we first monitored the processing and transport of the membrane protein Gas1p (Nuoffer et al., 1991). Because Gas1p undergoes a variety of posttranslational modifications during its biogenesis, defects at any stage can be detected by changes in gel mobility. Gas1p is initially synthesized in the cytosol as a 60-kD precursor that is detectable in protein translocation mutants (Ng et al., 1996). Upon entry into the ER, it is modified by N- and O-linked glycosylation, as well as by addition of a glycosylphosphatidylinositol (GPI) membrane anchor shifting its apparent molecular weight to 110 kD (Nuoffer et al., 1991). Gas1p folding occurs in the ER and requires the formation of intramolecular disulfide bonds (Frand and Kaiser, 1998). Only after correct folding can Gas1p continue to the Golgi apparatus ($t_{1/2} < 10$ min), where carbohydrate modification further changes its gel mobility to
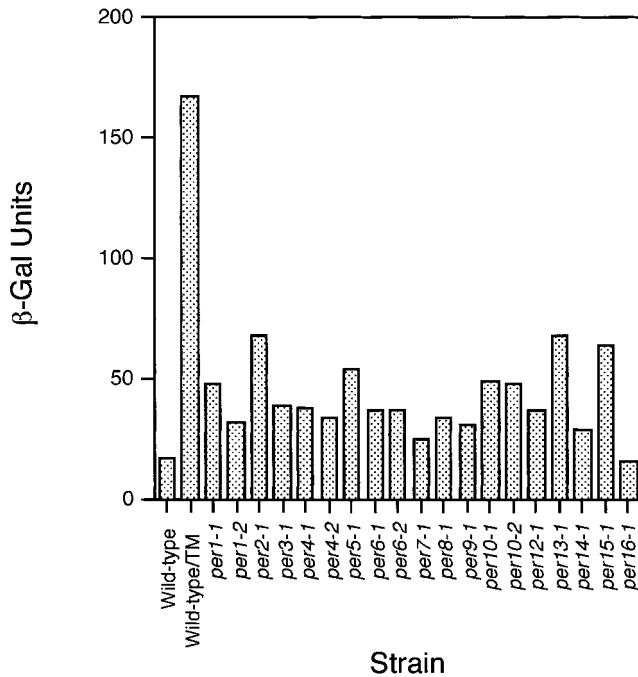
Figure 1. per mutants activate the unfolded protein response pathway. Wild-type and mutant cells carrying the *UPRE-LacZ* reporter gene are grown logarithmically and lysed. β-galactosidase activity is measured from lysates using 2-nitrophenyl-β-D-galactopyranoside (ONPG) as substrate and detected as an increase in absorbance at 420 nM. TM, cells treated with 2.5 μg/ml tunicamycin for 60 min before lysis.

125 kD (Nuoffer et al., 1991). Thus, defects in a variety of ER functions can be detected by monitoring Gas1p processing.

Wild-type (W303) and *per* mutant cells were metabolically pulse-labeled with [^{35}S]amino acids for five minutes and chased with an excess of unlabeled methionine and cysteine for 30 min to allow for full processing of Gas1p

(Fig. 2 A, lanes 2–22). As shown in Fig. 2, no preGas1p was observed in any lane, indicating that none of the *per* mutants displayed severe defects in protein translocation. However, about half of the mutants are defective in processing to the mature 125 kD form. These results indicate defects in ER protein processing functions that may include glycosylation, folding, GPI-anchor addition, or transport.

To distinguish the molecular nature of the observed defects further, we monitored the processing of another protein, the vacuolar protease CPY (Simons et al., 1995). The ER form of CPY is a core glycosylated proform (P1; Fig. 2 B, lane 1). The P1 form of CPY is transported to the Golgi apparatus, where it is modified by outer chain glycosylation to the P2 form. ProCPY is ultimately proteolytically processed to the mature form after transport to the vacuole (Fig. 2 B, lane 2). Underglycosylated CPY remains competent for folding and transport to the Golgi apparatus and vacuole. In the vacuole, it is processed to characteristic forms designated -1, -2, -3, -4 (te Heesen et al., 1992). Thus, based on specific gel mobility patterns, mutants defective for N-linked glycosylation can be easily distinguished.

As shown in Fig. 2 B, mutants *per3-1*, *per5-1*, *per6-1*, *per6-2*, *per12-1*, and *per14-1* exhibited CPY underglycoslyation indicative of defective N-linked glycosylation. Correspondingly, these mutants synthesized forms of Gas1p with altered mobility expected for glycosylation mutants (Fig. 2 A). The size of the underglycosylated forms indicates that most of CPY is proteolytically processed to the mature form in each of the mutants, indicating that these mutants are not generally defective in protein transport from the ER to the Golgi apparatus.

The PER5/RFT1 Gene Is a Novel UPR Target Required for N-linked Glycosylation

We chose to analyze *per5-1* in greater detail because it exhibited the most severe glycosylation defect. To this end, we analyzed CPY by pulse-chase analysis, followed by en-
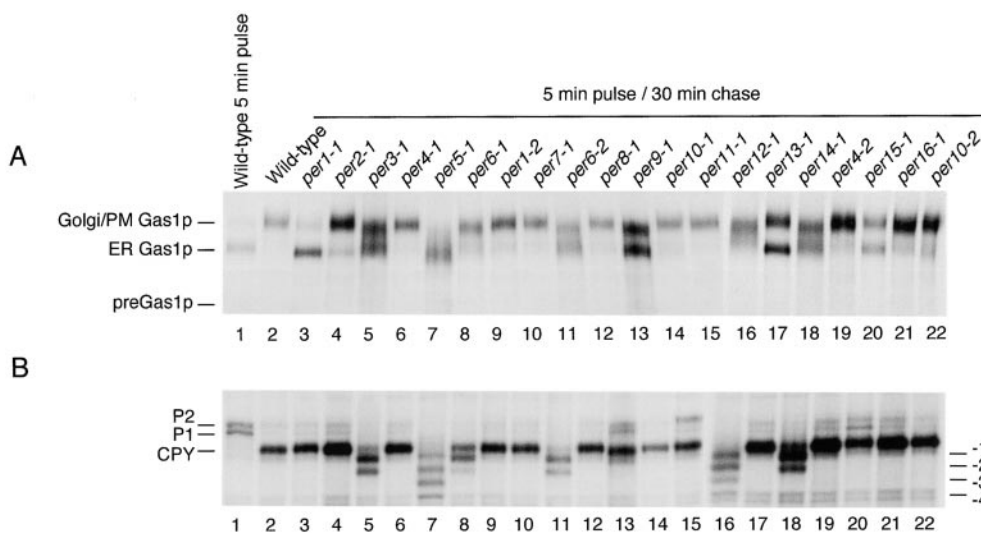

Figure 2. Processing of Gas1p and CPY in *per* mutants. Logarithmically growing wild-type and mutant cells were metabolically labeled with [^{35}S]methionine/cysteine for 5 min at 30°C, followed by a chase for 30 min. From detergent lysates, Gas1p and CPY were immunoprecipitated using monospecific polyclonal antisera. As a control, these proteins were also immunoprecipitated from wild-type lysates pulse-labeled with no chase to indicate the ER forms (lane 1). Proteins are separated on a 10–15% polyacrylamide gradient gel and visualized by fluorography. The positions of preGas1p, ER Gas1p, and Golgi/plasma membrane Gas1p (Golgi/PM) are indicated (A). For CPY, the ER (P1), Golgi apparatus (P2), and mature vacuolar form (CPY) are indicated to the left and the vacuolar underglycosylated forms (-1, -2, -3, -4) to the right of B.
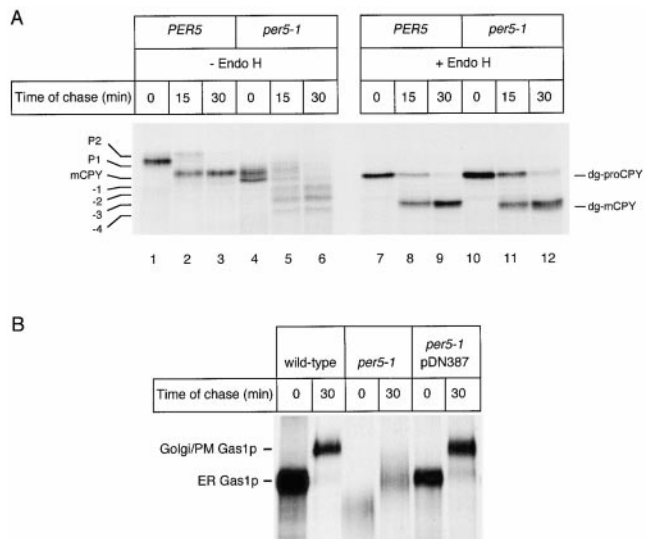
Figure 3. A, *per5-1* is defective in N-linked glycosylation. Wild-type (W303a) and *per5-1* cells were metabolically pulse-labeled for 5 min and chased for 0, 15, and 30 min. CPY was immunoprecipitated from detergent lysates and divided into two aliquots for each time point. One aliquot was treated with endoglycosidase H and the other was mock-treated. Proteins were separated on a 10% polyacrylamide gel and visualized by fluorography. The positions of the different pro and mature glycoforms of CPY are indicated as described in Fig. 2. Endo H deglycosylated pro (dg-proCPY) and mature forms (dg-mCPY) are indicated to the right. B, *per5-1* is an allele of *RFT1*. Wild-type, *per5-1*, and *per5-1* (pDN387) cells were pulse-labeled for 5 min and chased for 0 and 30 min. pDN387 is a centromeric vector containing the *RFT1* gene. Immunoprecipitates of Gas1p were resolved by a 10–15% polyacrylamide gradient gel and visualized by autoradiography. The normal ER and mature (Golgi/PM) forms are shown.

doglycosidase H digestion in wild-type and *per5-1* cells. As shown in Fig. 3 A, proCPY recovered after the pulse migrated as multiple species with altered mobility in *per5-1* cells as compared with the P1 species from wild-type cells (Fig. 3 A, compare lanes 1 and 4). Removal of the sugar chains revealed that the heterogeneity was exclusively due to differences in glycosylation, as the deglycosylated forms comigrated (Fig. 3 A, lanes 7–12). The kinetics of processing to the mature form(s) was similar in both strains, indicating that folding and transport functions are intact in *per5-1* cells. Similar results were obtained for Gas1p (Fig. 3 B), indicating that this defect is not substrate-specific.

To characterize the role of *PER5* further, we cloned the gene by complementation (see Materials and Methods). A complementing plasmid, pDN386, was isolated from transformed *per5-1* cells and portions of the insert further subcloned to identify the complementing gene. Plasmid pDN387, containing *RFT1* as the only open reading frame, fully complemented *per5-1* as it restored the sectoring phenotype and glycosylation function (Fig. 3 B). *RFT1* is an essential gene that encodes a predicted multispanning transmembrane protein of unknown function (Koerte et al., 1995). Thus, our approach identified *PER5/RFT1* as a novel gene required for N-linked glycosylation.

Inspection of the upstream sequences of *PER5/RFT1* revealed a potential UPRE, suggesting that transcription
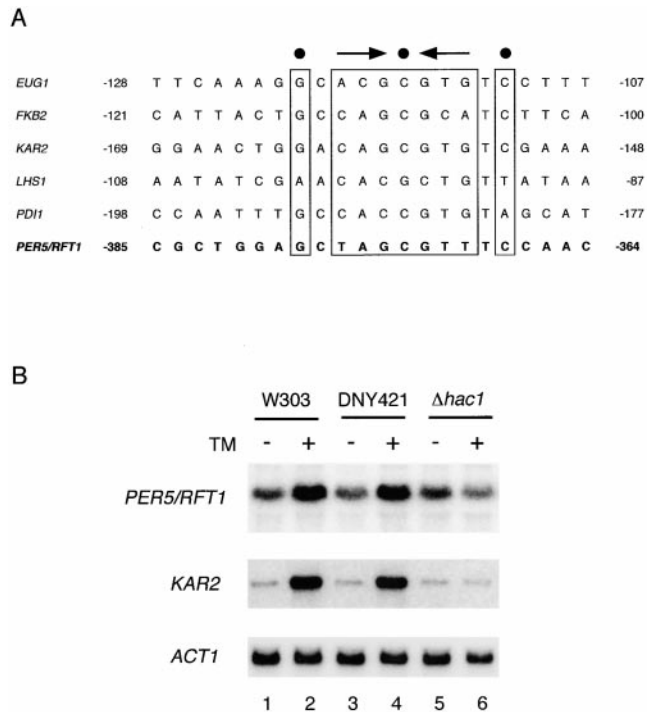

Figure 4. *PER5/RFT1* is a UPR target gene. A, Alignment of UPRE sequences. Experimentally determined UPRE sequences (Mori et al., 1998) are shown with an upstream sequence of *PER5/RFT1* that conforms to the palindromic motif shown by the arrows. Dots denote additional important positions in the motif. B, Northern analysis using RNA extracted from W303a, DNY421, and Δ*hac1* cells incubated in the presence or absence of 2.5 µg/ml of tunicamycin for 60 min at 30°C. *PER5/RFT1*, *KAR2*, and *ACT1* transcripts were blotted onto a nylon filter, hybridized to ^{32}P-labeled probes sequentially, and visualized by autoradiography. Quantification was performed by PhosphorImager analysis.

of *PER5* is regulated by the UPR (Fig. 4 A). To address this possibility directly, Northern analysis was performed using RNA extracted from control cells and from cells treated with the glycosylation inhibitor tunicamycin to induce UPR-regulated genes. As shown in Fig. 4 B, *PER5/RFT1* is elevated in tunicamycin-treated cells (lanes 1–4). Quantitative analysis showed a moderate 2.5-fold induction. This is in contrast to *KAR2*, which was induced over 8-fold (Fig. 4 B). Transcriptional regulation of *PER5/RFT1*, as with *KAR2*, was dependent on the UPR, as no induction was detected in Δ*hac1* cells (Fig. 4 B, lanes 5 and 6).

Taken together, the analyses in Figs. 2–4 show that mutations in at least 5 of 16 *PER* genes compromise important functions in protein glycosylation and that genes of heretofore unknown function have been identified in this way. Moreover, these results reinforce the notion that the UPR functions to regulate a variety of aspects of protein biogenesis.

A Role for the UPR in ERAD

As many of the *per* mutants do not exhibit defects in Gas1p or CPY maturation, we wondered whether other aspects of ER function related to protein maturation are affected in some of the *per* mutants. To test whether
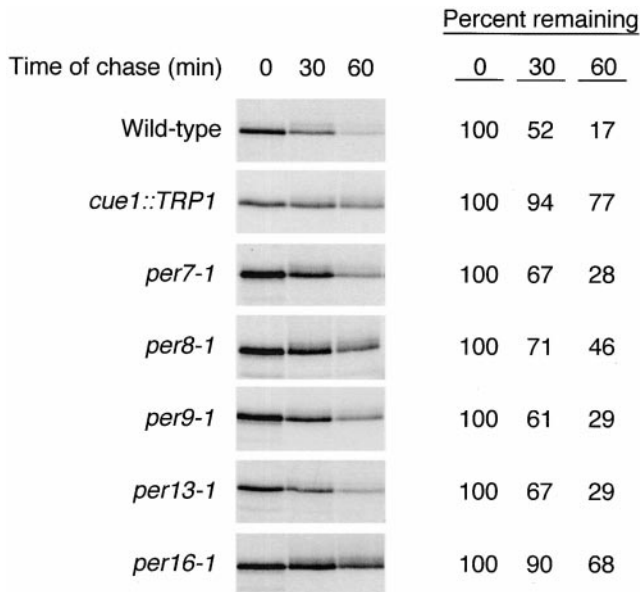
	Percent remaining		
Time of chase (min)	0	30	60
Wild-type	100	52	17
cue1::TRP1	100	94	77
per7-1	100	67	28
per8-1	100	71	46
per9-1	100	61	29
per13-1	100	67	29
per16-1	100	90	68

Figure 5. A subset of *per* mutants is defective for ERAD. All twenty *per* mutants were transformed with pDN436 (CPY*$_{HA}$) and pulse-chase analysis performed to measure the degradation of the ERAD substrate CPY*$_{HA}$. Immunoprecipitates of CPY*$_{HA}$ were normalized using TCA precipitable counts. The proteins were separated by PAGE followed by autoradiography. Quantification was performed by PhosphorImager analysis and reported as percent remaining to the right of each respective autoradiogram. In addition to the wild-type (DNY563) and ERAD mutant (DNY572, *cue1::TRP1*) controls, only *per* mutants with significant ERAD defects are shown.

genes encoding ERAD components were identified in this screen, we constructed a recombinant form of the ERAD substrate, CPY* (Finger et al., 1993), modified by addition of an HA epitope tag to simplify analysis. The new version, designated CPY*$_{HA}$, behaved as a proper ERAD substrate: it was degraded rapidly in wild-type cells and was stabilized in a strain lacking the ERAD gene, *CUE1* (Fig. 5; Biederer et al., 1997). We transformed each of the *per* mutants with pDN436, carrying the gene encoding CPY*$_{HA}$. Pulse-chase analysis was used to assess substrate stability in each strain. Turnover of CPY*$_{HA}$ was delayed in *per7-1*, *per8-1*, *per9-1*, *per13-1*, and *per16-1* (Fig. 5). Two mutants, *per9-1* and *per13-1*, also displayed defects in Gas1p processing, indicating that their defects are pleiotropic. Their ERAD phenotypes may therefore be indirect. In all other *per* strains, including those displaying severely impaired protein processing, the rate of CPY*$_{HA}$ degradation was not altered (data not shown).

We next cloned some of the affected genes of *per* mutants displaying ERAD defects, starting with *PER8* and *PER16*, which displayed defects similar in extent to the Δ*cue1* strain. Plasmid pDN426 bearing *SON1*, completely complemented the *per8-1* mutant. Moreover, CPY*$_{HA}$ was stabilized in Δ*son1* cells (data not shown), indicating that the defect *per8-1* cells reflects a loss-of-function. Son1p was recently shown to be a transcription factor that regulates proteasome biogenesis (Mannhaupt et al., 1999), and Δ*son1* mutants are defective in cytosolic protein degrada-
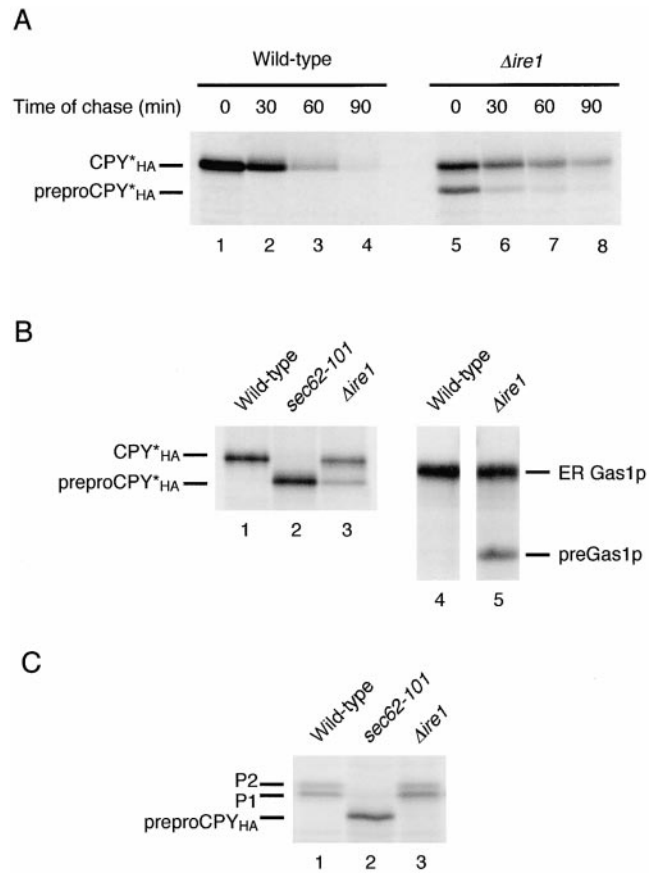

Figure 6. The UPR is required for efficient ER protein translocation and ERAD. A, Wild-type and *ire1::TRP1* cells (labeled Δ*ire1*) expressing CPY*$_{HA}$ were pulse-labeled for 10 min with [^{35}S]methionine/cysteine and chased for 0, 30, 60, and 90 min. CPY*$_{HA}$ was immunoprecipitated using anti-HA mAb and analyzed by SDS-PAGE. The proteins were visualized by direct autoradiography and quantification of the gel was performed using a PhosphorImager. B, Wild-type, *sec62-101*, and Δ*ire1* cells expressing CPY*$_{HA}$ were pulse-labeled for 10 min and CPY*$_{HA}$ immunoprecipitated and separated on a 10% polyacrylamide gel (lanes 1, 2, and 3). Lanes 4 and 5, Gas1p immunoprecipitated from the lysates used for lanes 1 and 3. C, Wild-type, *sec62-101*, and Δ*ire1* cells expressing CPY$_{HA}$ were pulse-labeled for 10 min and immunoprecipitated for endogenous CPY. The position of preproCPY$_{HA}$, the ER P1, and Golgi P2 forms are indicated.

tion (Johnson et al., 1995). Thus, a role for Son1p in ERAD is quite plausible.

We cloned *PER16* by screening for restoration of the sectoring phenotype after a plasmid shuffle of the *URA3*-marked reporter for *LEU2* (pDN388) and transformation of the library. Subcloning of the inserts of plasmids that restored the sectoring phenotype of *per16-1* cells identified *UBC7*, which was sufficient to complement the *per16-1* mutation. *UBC7* encodes a ubiquitin-conjugating enzyme that was previously shown to participate in ERAD (Biederer et al., 1996; Hiller et al., 1996).

The isolation of ERAD mutants in this screen suggested a tight physiological link between the UPR and ERAD. We explored this notion further by monitoring the fate of CPY*$_{HA}$ in a UPR-deficient strain. As shown in Fig. 6 A,

CPY*$_{HA}$ was stabilized in Δ*ire1* cells (Fig. 6 A, lanes 5–8), whereas wild-type control cells degraded the substrate rapidly. Surprisingly, we also observed the appearance of a faster migrating band in Δ*ire1* cells that was not detected in control experiments performed with wild-type cells (Fig. 6 A, labeled preproCPY*$_{HA}$). Its mobility and the timing of its appearance during the pulse suggested that the band represents the cytoplasmic, nontranslocated preproCPY*$_{HA}$. To confirm this identity, we expressed CPY*$_{HA}$ in *sec62-101* cells, in which translocation of CPY is severely impaired and thus accumulated cytosolic precursor proteins. The data in Fig. 6 B show that the preproCPY bands comigrate (compare lanes 2 and 3).

These results raised the question whether impaired translocation resulted from the synthesis of misfolded protein or from an increased flux of proteins through the ER translocon due to ectopic expression of CPY*$_{HA}$. To distinguish between these possibilities, we constructed wild-type and Δ*ire1* strains to express epitope-tagged wild-type CPY (CPY$_{HA}$) using the same vector as for CPY*$_{HA}$. Expression of CPY$_{HA}$ caused no translocation defects in Δ*ire1* cells (Fig. 6 C), indicating that the defect results specifically from the expression of a misfolded protein that is a substrate of the ERAD pathway.

In Δ*ire1* cells expressing CPY*$_{HA}$, we also observed a translocation defect for the endogenous protein Gas1p (Fig. 6 B, lanes 4 and 5), suggesting that the misfolded protein causes a general translocation defect in these cells. By contrast, Δ*ire1* cells alone or Δ*ire1* cells expressing CPY$_{HA}$ exhibit no defects in ER import of Gas1p (data not shown). As protein import into and export from the ER are thought to share the same translocation pore, it is possible that both processes directly compete for some limiting component(s) regulated by the UPR.

Quantitative analysis of the data in Fig. 6 A showed a delay of ER protein degradation in Δ*ire1* cells. In wild-type cells, 47, 13, and 3% of CPY*$_{HA}$ remained after 30, 60, and 90 minutes of chase, respectively. By contrast, in Δ*ire1* cells, 46, 37, and 22% of CPY*$_{HA}$ remained at the corresponding time points. This delay could result from two, possibly additive, effects: an impairment of import into the ER and a delay in reexport from the ER for degradation. Although the relative contributions of the two processes to the overall delay remains to be determined, ERAD function remains disrupted if the import block is alleviated (see below).

Taken together, the data suggest a role of the UPR in balancing the trafficking of proteins into and out of the ER during periods of stress as import and export substrates compete for a limiting core translocation machinery. The accumulation of CPY*$_{HA}$ would induce the UPR to augment the translocation machinery to clear the ER of the misfolded proteins while maintaining protein import into the ER. In support of this hypothesis, genes encoding components of the translocation machinery with roles for both import and export are targets of the UPR (Travers et al., 2000). In addition, CPY* and CPY*$_{HA}$ expression each cause UPR induction, albeit at a modest level of less than twofold as measured by a *UPRE-lacZ* reporter (Knop et al., 1996; Spear, E.D., and D.T.W. Ng, unpublished results).

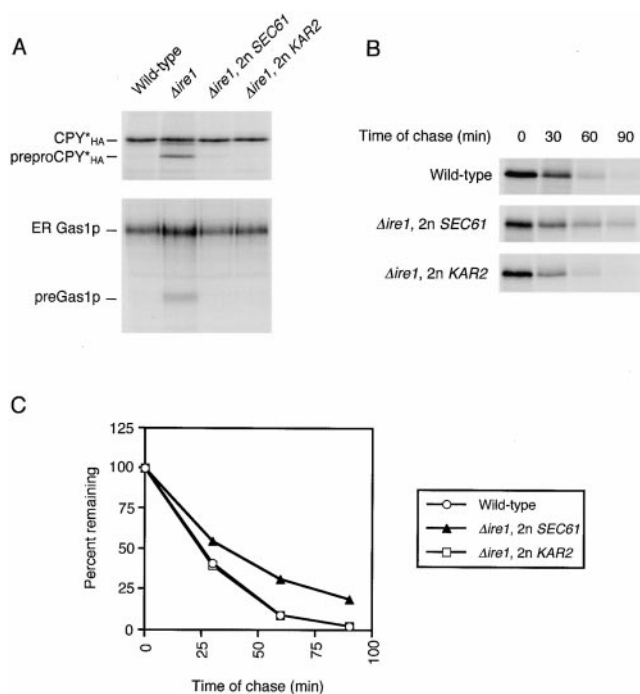To test this hypothesis, we assessed the contribution of

Figure 7. Increased gene dosage of specific UPR targets alleviate translocation and ERAD defects in UPR-deficient cells. A, Wild-type and Δ*ire1* cells expressing CPY*$_{HA}$ were pulse-labeled with [^{35}S]methionine/cysteine followed by immunoprecipitation for CPY*$_{HA}$ (top) and Gas1p (bottom). Haploid strains DNY563 (wild-type), ESY157 (Δ*ire1*), ESY158 (ESY157 with an extra copy of *KAR2* on the centromeric plasmid pMR713; labeled Δ*ire1*, 2n *KAR2*), and ESY159 (ESY157 with and extra copy of *SEC61* on the centromeric plasmid pCS15; labeled Δ*ire1*, 2n *SEC61*) were analyzed. The lumenal and nontranslocated forms (pre) are indicated. B, DNY563 (wild-type), ESY158 (Δ*ire1*, 2n *KAR2*), and ESY159 (Δ*ire1*, 2n *SEC61*) cells were pulse-labeled with [^{35}S]methionine/cysteine for 10 min, followed by a cold chase for the times indicated, CPY*$_{HA}$ immunoprecipitated from detergent lysates, and separated by SDS-PAGE. C, Quantification of immunoprecipitated CPY*$_{HA}$ shown in B by PhosphorImager analysis.

two specific UPR target genes by increasing their expression as it would occur during normal UPR activation. To this end, we tested strains that contain duplicated genes encoding Kar2p or Sec61p, respectively. These genes were selected because of their dual roles in both ER protein import and ERAD (Pilon et al., 1997; Plemper et al., 1997; Zhou and Schekman, 1999). In addition, both genes are inducible under conditions that activate the UPR (Travers et al., 2000). As shown in Fig. 7 A, increased gene dosage of either Kar2p or Sec61p was sufficient to alleviate the translocation defect for preproCPY*$_{HA}$ and preGas1p in Δ*ire1* cells. Δ*ire1* cells with increased expression of Kar2p also alleviated the delay in CPY*$_{HA}$ degradation (Fig. 7, B and C). In contrast, Δ*ire1* cells containing an additional copy of *SEC61* remain defective in degrading CPY*$_{HA}$. The additional copy of *SEC61* itself is not inhibitory to ERAD since wild-type cells under the same circumstances show normal if slightly accelerated ERAD function (Spear, E.D., and D.T.W. Ng, unpublished results). These results show that Kar2p becomes limiting for both translocation

and ERAD when cells are challenged with CPY*$_{HA}$, whereas Sec61p becomes limiting only for translocation, but not ERAD. Moreover, increased expression of either Kar2p or Sec61p can compensate for the translocation defect in $\Delta ire1$ cells. Taken together, these data demonstrate an important role for the UPR in regulating the import and export functions across the ER membrane.

The UPR Controls a Wide Variety of ER Functions

As described so far, the genetic approach has revealed two new functions, ERAD and glycosylation, that, when limiting, require activation of the unfolded protein response for cell viability. In addition, cloning of *per13* and *per2* revealed that the mutations map to *GPI10* and *MCD4*, respectively, both encoding essential components in GPI anchor addition. As *MCD4*, other genes required for GPI biosynthesis, including *GAA1*, *GPI12*, and *LAS21* are also regulated by the UPR (Travers et al., 2000); *GPI10*, in contrast, was not identified as a UPR transcriptional target gene. Finally, cloning of *per4* revealed that the mutation resides in *LHS1/SSI1*, an hsp70-like ER chaperone (Baxter et al., 1996; Craven et al., 1996), thus adding to the list of classical UPR targets that mediate protein folding directly. Consistent with previous observations, the *per4* mutants display a minor protein translocation defect following a short pulse label (data not shown). Thus, genetic analysis reveals a wide variety of ER functions that are physiologically linked to the UPR.

Discussion

Characterization of the *per* mutants revealed that cells require a functional UPR to cope with and compensate for defects in many aspects of protein maturation in the ER, including protein folding, glycosylation, and GPI anchor addition. In addition, we found that ERAD, required to clear the ER of unwanted proteins, is intimately linked to the UPR. A gene expression chip analysis performed in a parallel study to determine the transcriptional scope of the UPR revealed that over 350 genes are transcriptionally upregulated upon induction of the pathway (Travers et al., 2000). Many of the identified genes function in various aspects of the secretory pathway at the level of the ER or beyond. Thus, together the results of the two studies show that the role of the UPR is multifaceted and much more complex than previously appreciated. Importantly, not all of the genes identified as *per* mutants are transcriptional targets of the UPR. Genetic and gene expression array analyses therefore proved complementary rather than redundant approaches, with both avenues allowing the identification of novel genes that function in these processes.

Regulation of Protein Glycosylation

Isolation of the *per5-1* mutant led to the discovery of a new gene involved in protein glycosylation. We found that *PER5* is upregulated by the UPR. *PER5/RFT1* was originally cloned from a yeast mutant requiring the overexpressing of human p53 for viability (Koerte et al., 1995); as there is no yeast equivalent to mammalian p53, the reason for this phenotype and the function of *PER5/RFT1* has remained obscure. Our studies demonstrate that *PER5/*

RFT1 is required for efficient N-linked glycosylation of glycoproteins. *PER5/RFT1* encodes a multispanning transmembrane protein that bears no significant sequence similarity to any other known component of the glycosylation machinery. Our results suggest that *PER5/RFT1* functions in biosynthesis of the dolichol-linked carbohydrate precursor or in the protein conjugation step. Preliminary experiments indicate that *per5-1* cells show an accumulation of a biosynthetic intermediate (Dol-PP-GlcNAc$_2$-Man$_5$) and a sharp decrease in the mature form (Dol-PP-GlcNAc$_2$-Man$_9$-Glc$_3$; J. Helenius, D.T.W. Ng, P. Walter, and M. Aebi, unpublished results). These results suggest the intriguing possibility that *PER5/RFT1* may encode the long sought-after flippase that translocates the Dol-PP-GlcNAc$_2$-Man$_5$ intermediate (which is synthesized on the cytosolic face of the membrane) to the lumenal face for further processing (Burda and Aebi, 1999). Consistent with this view, those carbohydrates that are attached to proteins in *per5-1* cells were found to be fully mature. Further experiments to address this notion are in progress.

Genome expression data has shown that additional components of the glycosylation biosynthetic machinery are regulated by the UPR (Travers et al., 2000). The regulation of glycosylation components helps cement our broadened view of the UPR, as it indicates a role of the pathway in adjusting the cell's biosynthetic capacity of the ER according to need. Similarly, we isolated *per* mutants defective in GPI anchorage, and many GPI biosynthetic genes are UPR targets (Travers et al., 2000).

UPR Regulation of ER Quality Control

The identification of ERAD genes suggested a tight physiological link between ERAD and the UPR. We have provided direct evidence for such a link using CPY*$_{HA}$, which is stabilized in UPR-deficient cells. Consistent with previous studies (Kawahara et al., 1997; Zhou and Schekman, 1999), we show that various ERAD-deficient mutants constitutively induce the UPR. As shown in the parallel study, most known ERAD genes are activated by the UPR (Travers et al., 2000). Moreover, in this study we have shown that UPR induction increases ERAD efficiency. Thus the UPR and ERAD are intimately coordinated and interdependent.

The identification of *SON1* (*PER8*) as a gene required for ERAD provided an unexpected twist to the outcome of our genetic screen. *SON1* (also called *RPN4*) was recently shown to be a transcriptional activator that binds a consensus promoter element, termed PACE (Mannhaupt et al., 1999). The PACE motif is found in many genes, but is a common element in the family of genes encoding subunits of the 26S proteasome. In *son1* null mutants, the degradation of some cytosolic proteins are impaired at a step following ubiquitin conjugation (Johnson et al., 1995). Together, these data suggest *SON1* regulates aspects of proteasome biogenesis, which in turn is required for ERAD. Surprisingly however, neither *SON1* nor proteasomal subunit genes are regulated by the UPR (Travers et al., 2000). Rather, proteasomal subunit genes are coordinately upregulated in UPR-deficient cells following treatment with tunicamycin or DTT (Travers et al., 2000). These results suggest that, in addition to the UPR, a UPR-independent

ER → nucleus signal transduction pathway exists in which Son1p may play an important role. Interestingly, the UPR target genes *PDI1* and *PER5/RFT1* contain consensus PACE promoter elements (Mannhaupt et al., 1999), and may hence be regulated by Son1p, in addition to Hac1p.

Regulation of Protein Translocation Into and Out of the ER

The observation that UPR-deficient cells expressing CPY*$_{HA}$ exhibit general protein translocation defects revealed another unexpected role for the UPR. As discussed above, our analyses show a delay in the degradation of CPY*$_{HA}$ via ERAD. We consider it likely that these two phenomena are linked as several components of the ER translocon are thought to be both required protein import and export (Wiertz et al., 1996; Pilon et al., 1997; Plemper et al., 1997): UPR-regulated factors shared between import and export may become limiting under conditions as an extra load of an ERAD substrate needs to be attended to.

We confirmed this notion by testing two UPR target genes with known roles in translocation for import and export by increasing their gene dosage. We found that an extra copy of *SEC61* was sufficient to alleviate the import defect, but degradation was still compromised (Fig. 7), while an extra copy of *KAR2* restored both import and ERAD functions. These results suggest that primarily Kar2p becomes limiting under these conditions. Interestingly, expression of the mouse major histocompatability complex class I heavy chain H-2Kb in yeast also displayed rapid ER degradation that is dependent on UPR function (Casagrande et al., 2000). In apparent contrast to our results, Kar2p overexpression showed no improvement of heavy chain degradation in Δ*ire1* cells. We also observed, however, that more dramatic overexpression of Kar2p can actually inhibit the degradation of CPY*$_{HA}$ in wild-type cells (Spear, E.D., and D.T.W. Ng, unpublished results; J. Brodsky, personal communication). Taken together, these data suggest that a precise and balanced modulation of UPR targets is required for optimal ERAD activity.

These results serve to illustrate a simple approach that possibly can be more broadly exploited to study pathways under UPR control. Starting with a UPR-deficient strain, one imposes a specific nonlethal stress that in wild-type cells would elicit a moderate UPR induction (in this case, moderate CPY*$_{HA}$ expression). With the UPR off, key components become limiting. As defects are detected, it becomes possible to test the contribution of specific UPR target genes by increasing their gene dosage. Only some of many genes required for any given function are regulated by the UPR (Travers et al., 2000) which, we surmise, are likely to comprise those components that are rate limiting under uninduced conditions. Thus, the approach may allow to identify key regulatory components even for processes that require the contribution of multiple genes.

References

Baxter, B.K., P. James, T. Evans, and E.A. Craig. 1996. *SSI1* encodes a novel Hsp70 of the *Saccharomyces cerevisiae* endoplasmic reticulum. *Mol. Cell. Biol.* 16:6454–6456.

Biederer, T., C. Volkwein, and T. Sommer. 1996. Degradation of subunits of the Sec61p complex, an integral component of the ER membrane, by the ubiquitin–proteasome pathway. *EMBO (Eur. Mol. Biol. Organ.) J.* 15:2069–2076.

Biederer, T., C. Volkwein, and T. Sommer. 1997. Role of Cue1p in ubiquitination and degradation at the ER surface. *Science.* 278:1806–1809.

Boeke, J.D., F. LaCroute, and G.R. Fink. 1984. A positive selection for mutants lacking orotidine-5′-phosphate decarboxylase activity in yeast: 5-fluoro-orotic acid resistance. *Mol. Gen. Genet.* 197:345–346.

Brodsky, J.L., and A.A. McCracken. 1999. ER protein quality control and proteasome-mediated protein degradation. *Sem. Cell Dev. Biol.* 10:501–513.

Burda, P., and M. Aebi. 1999. The dolichol pathway of N-linked glycosylation. *Biochim. Biophys. Acta.* 1426:239–257.

Casagrande, R., P. Stern, M. Diehn, C. Shamu, M. Osario, M. Zuniga, P. Brown, and H. Ploegh. 2000. Degradation of proteins from the ER of *S. cerevisiae* requires an intact unfolded protein response pathway. *Mol. Cell.* 5:729–735.

Chapman, R.E., and P. Walter. 1997. Translational attenuation mediated by an mRNA intron. *Curr. Biol.* 7:850–859.

Chapman, R., C. Sidrauski, and P. Walter. 1998. Intracellular signaling from the endoplasmic reticulum to the nucleus. *Annu. Rev. Cell. Dev. Biol.* 14:459–485.

Cox, J., and P. Walter. 1996. A novel mechanism for regulating activity of a transcription factor that controls the unfolded protein response. *Cell.* 87:391–404.

Cox, J.S., C.E. Shamu, and P. Walter. 1993. Transcriptional induction of genes encoding ER resident proteins requires a transmembrane protein kinase. *Cell.* 73:1197–1206.

Cox, J.S., R.E. Chapman, and P. Walter. 1997. The unfolded protein response coordinates the production of endoplasmic reticulum protein and endoplasmic reticulum membrane. *Mol. Biol. Cell.* 8:1805–1814.

Craven, R.A., M. Egerton, and C.J. Stirling. 1996. A novel Hsp70 of the yeast ER lumen is required for the efficient translocation of a number of protein precursors. *EMBO (Eur. Mol. Biol. Organ.) J.* 15:2640–2650.

Finger, A., M. Knop, and D.H. Wolf. 1993. Analysis of two mutated vacuolar proteins reveals a degradation pathway in the endoplasmic reticulum or a related compartment of yeast. *Eur. J. Biochem.* 218:565–574.

Frand, A.R., and C.A. Kaiser. 1998. The *ERO1* gene of yeast is required for oxidation of protein dithiols in the endoplasmic reticulum. *Mol. Cell.* 1:161–170.

Guthrie, C., and G.R. Fink. 1991. Guide to yeast genetics and molecular biology. *In* Methods in Enzymology. J.N. Abelson and M.I. Simon, editors. Academic Press, Inc. San Diego, CA. 933 pp.

Hiller, M.M., A. Finger, M. Schweiger, and D.H. Wolf. 1996. ER degradation of a misfolded luminal protein by the cytosolic ubiquitin–proteasome pathway. *Science.* 273:1725–1728.

Johnson, E.S., P.C. Ma, I.M. Ota, and A. Varshavsky. 1995. A proteolytic pathway that recognizes ubiquitin as a degradation signal. *J. Biol. Chem.* 270:17442–17456.

Kaufman, R.J. 1999. Stress signaling from the lumen of the endoplasmic reticulum: coordination of gene transcriptional and translational controls. *Genes Dev.* 13:1211–1233.

Kawahara, T., H. Yanagi, T. Yura, and K. Mori. 1997. Endoplasmic reticulum stress-induced mRNA splicing permits synthesis of transcription factor Hac1p/Ern4p that activates the unfolded protein response. *Mol. Biol. Cell.* 8:1845–1862.

Knop, M., A. Finger, T. Braun, K. Hellmuth, and D.H. Wolf. 1996. Der1, a novel protein specifically required for endoplasmic reticulum degradation in yeast. *EMBO (Eur. Mol. Biol. Organ.) J.* 15:753–763.

Koerte, A., T. Chong, X. Li, K. Wahane, and M. Cai. 1995. Suppression of the yeast mutation rft1–1 by human p53. *J. Biol. Chem.* 270:22556–22564.

Kohno, K., K. Normington, J. Sambrook, M.J. Gething, and K. Mori. 1993. The promoter region of the yeast KAR2 (BiP) gene contains a regulatory domain that responds to the presence of unfolded proteins in the endoplasmic reticulum. *Mol. Cell. Biol.* 13:877–890.

Koshland, D., J.C. Kent, and L.H. Hartwell. 1985. Genetic analysis of the mitotic transmission of minichromosomes. *Cell.* 40:393–403.

Kozutsumi, Y., M. Segal, K. Normington, M.J. Gething, and J. Sambrook. 1988. The presence of malfolded proteins in the endoplasmic reticulum signals the induction of glucose-regulated proteins. *Nature.* 332:462–464.

Lagosky, P.A., G.R. Taylor, and R.H. Haynes. 1987. Molecular characterization of the *Saccharomyces cerevisiae* dihydrofolate reductase gene (DFR1). *Nucleic Acids Res.* 15:10355–10371.

LaMantia, M., T. Miura, H. Tachikawa, H.A. Kaplan, W.J. Lennarz, and T. Mizunaga. 1991. Glycosylation site binding protein and protein disulfide

isomerase are identical and essential for cell viability in yeast. *Proc. Natl. Acad. Sci. USA.* 88:4453–4457.

Mannhaupt, G., R. Schnall, V. Karpov, I. Vetter, and H. Feldmann. 1999. Rpn4p acts as a transcription factor by binding to PACE, a nonamer box found upstream of 26S proteasomal and other genes in yeast. *FEBS Lett.* 450:27–34.

Mori, K., A. Sant, K. Kohno, K. Normington, M.J. Gething, and J.F. Sambrook. 1992. A 22 bp cis-acting element is necessary and sufficient for the induction of the yeast KAR2 (BiP) gene by unfolded proteins. *EMBO (Eur. Mol. Biol. Organ.) J.* 11:2583–2593.

Mori, K., W. Ma, M.J. Gething, and J. Sambrook. 1993. A transmembrane protein with a cdc2[+]/CDC28-related kinase activity is required for signaling from the ER to the nucleus. *Cell.* 74:743–756.

Mori, K., T. Kawahara, H. Yoshida, H. Yanagi, and T. Yura. 1996. Signalling from endoplasmic reticulum to nucleus: transcription factor with a basic-leucine zipper motif is required for the unfolded protein-response pathway. *Genes Cells.* 1:803–817.

Mori, K., N. Ogawa, T. Kawahara, H. Yanagi, and T. Yura. 1998. Palindrome with spacer of one nucleotide is characteristic of the cis-acting unfolded protein response element in *Saccharomyces cerevisiae. J. Biol. Chem.* 273:9912–9920.

Ng, D.T.W., J.D. Brown, and P. Walter. 1996. Signal sequences specify the targeting route to the endoplasmic reticulum membrane. *J. Cell Biol.* 134:269–278.

Nikawa, J.I., and S. Yamashita. 1992. *IRE1* encodes a putative protein kinase containing a membrane-spanning domain and is required for inositol prototrophy in *Saccharomyces cerevisiae. Mol. Microbiol.* 6:1441–1446.

Normington, K., K. Kohno, Y. Kozutsumi, M.J. Gething, and J. Sambrook. 1989. *S. cerevisiae* encodes an essential protein homologous in sequence and function to mammalian BiP. *Cell.* 57:1223–1236.

Nunnari, J., and P. Walter. 1996. Regulation of organelle biogenesis. *Cell.* 84:389–394.

Nuoffer, C., P. Jeno, A. Conzelmann, and H. Riezman. 1991. Determinants for glycophospholipid anchoring of the *Saccharomyces cerevisiae* GAS1 protein to the plasma membrane. *Mol. Cell. Biol.* 11:27–37.

Partaledis, J.A., and V. Berlin. 1993. The FKB2 gene of *Saccharomyces cerevisiae*, encoding the immunosuppressant-binding protein FKBP-13, is regulated in response to the accumulation of unfolded proteins in the endoplasmic reticulum. *Proc. Natl. Acad. Sci. USA.* 90:5450–5454.

Pilon, M., R. Schekman, and K. Romisch. 1997. Sec61p mediates export of a misfolded secretory protein from the endoplasmic reticulum to the cytosol for degradation. *EMBO (Eur. Mol. Biol. Organ.) J.* 16:4540–4548.

Plemper, R.K., S. Bohmler, J. Bordallo, T. Sommer, and D.H. Wolf. 1997. Mutant analysis links the translocon and BiP to retrograde protein transport for ER degradation. *Nature.* 388:891–895.

Pollard, M.G., K.J. Travers, and J.S. Weissman. 1998. Ero1p: a novel and ubiquitous protein with an essential role in oxidative protein folding in the endoplasmic reticulum. *Mol. Cell.* 1:171–182.

Pouyssegur, J., R.P.C. Shiu, and I. Pastan. 1977. Induction of transformation-sensitive membrane polypeptides in normal fibroblasts by a block in glycoprotein synthesis or glucose deprivation. *Cell.* 11:941–947.

Rose, M.D., P. Novick, J.H. Thomas, D. Botstein, and G.R. Fink. 1987. A *Saccharomyces cerevisiae* genomic plasmid bank based on a centromere-containing shuttle vector. *Gene.* 60:237–243.

Rose, M.D., L.M. Misra, and J.P. Vogel. 1989. KAR2, a karyogamy gene, is the yeast homolog of the mammalian BiP/GRP78 gene. *Cell.* 57:1211–1221.

Shamu, C.E., and P. Walter. 1996. Oligomerization and phosphorylation of the Ire1p kinase during intracellular signaling from the endoplasmic reticulum to the nucleus. *EMBO (Eur. Mol. Biol. Organ.) J.* 15:3028–3039.

Sidrauski, C., J.S. Cox, and P. Walter. 1996. tRNA ligase is required for regulated mRNA splicing in the unfolded protein response. *Cell.* 87:405–413.

Sikorski, R.S., and P. Hieter. 1989. A system of shuttle vectors and yeast host strains designed for efficient manipulation of DNA in *Saccharomyces cerevisiae. Genetics.* 122:19–27.

Simons, J.F., S. Ferro-Novick, M.D. Rose, and A. Helenius. 1995. BiP/Kar2p serves as a molecular chaperone during carboxypeptidase Y folding in yeast. *J. Cell Biol.* 130:41–49.

Sommer, T., and D.H. Wolf. 1997. Endoplasmic reticulum degradation: reverse protein flow of no return. *FASEB J.* 11:1227–1233.

Stearns, T., and D. Botstein. 1988. Unlinked noncomplementation: isolation of new conditional-lethal mutations in each of the tubulin genes of *Saccharomyces cerevisiae. Genetics.* 119:249–260.

Tachibana, C., and T.H. Stevens. 1992. The yeast *EUG1* gene encodes an endoplasmic reticulum protein that is functionally related to protein disulfide isomerase. *Mol. Cell Biol.* 12:4601–4611.

te Heesen, S., B. Janetzky, L. Lehle, and M. Aebi. 1992. The yeast *WBP1* is essential for oligosaccharyltransferase activity in vivo and in vitro. *EMBO (Eur. Mol. Biol. Organ.) J.* 11:2071–2075.

Travers, K.J., C.K. Patil, L. Wodicka, D.J. Lockhart, J.S. Weissman, and P. Walter. 2000. Functional and genomic analysis reveal essential coordination between the unfolded protein response and endoplasmic reticulum-associated degradation. *Cell.* 101:249–258.

Wiertz, E.J., D. Tortorella, M. Bogyo, J. Yu, W. Mothes, T.R. Jones, T.A. Rapoport, and H.L. Ploegh. 1996. Sec61-mediated transfer of a membrane protein from the endoplasmic reticulum to the proteasome for destruction. *Nature.* 384:432–438.

Zhou, M., and R. Schekman. 1999. The engagement of Sec61p in the ER dislocation process. *Mol. Cell.* 4:925–934.